Inorganic Chemistry

ARTICLE

pubs.acs.org/IC

Modulating the Photophysical Properties of Azamacrocyclic Europium Complexes with Charge-Transfer Antenna Chromophores

Adrien Bourdolle,[†] Mustapha Allali,[‡] Jean-Christophe Mulatier,[†] Boris Le Guennic,[†] Jurriaan M. Zwier,[‡] Patrice L. Baldeck,[§] Jean-Claude G. Bünzli,[⊥] Chantal Andraud,[†] Laurent Lamarque,*[,‡] and Olivier Maury*[,†]

[‡]Cisbio Bioassays, Parc Marcel Boiteux, BP 84175, 30204 Bagnols-sur-Cèze Cedex, France

[†]Université de Lyon 1, CNRS UMR 5182, Ecole Normale Supérieure de Lyon, 46 allée d'Italie, 69007 Lyon, France

[§]Laboratoire de Spectrométrie Physique, Université Joseph Fourier, CNRS UMR 5588, BP 87, F-38402 Saint Martin d'Hères, France

[⊥]Institute of Chemical Sciences and Engineering, École Polytechnique Fédérale de Lausanne, BCH 1402, CH-1015 Lausanne, Switzerland

Supporting Information

ABSTRACT:

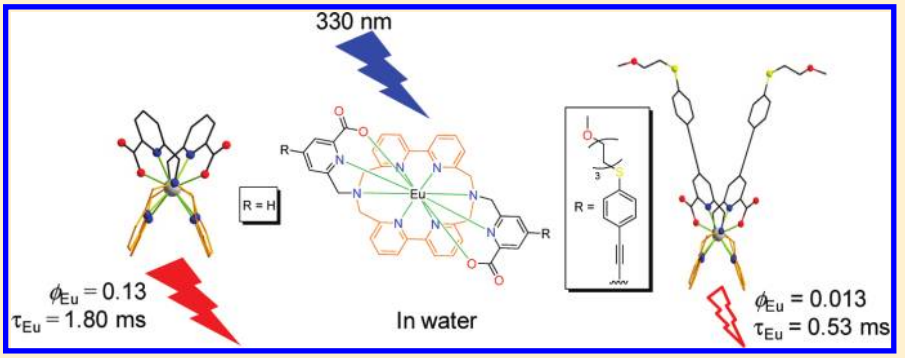

Two europium complexes with bis(bipyridine) azamacrocyclic ligands featuring pendant arms with or without π-conjugated donor groups are synthesized and fully characterized by theoretical calculations and NMR spectroscopy. Their photophysical properties, including two-photon absorption, are investigated in water and in various organic solvents. The nonfunctionalized ligand gives highly water-stable europium complexes featuring bright luminescence properties but poor two-photon absorption cross sections. On the other hand, the europium complex with an extended conjugated antenna ligand presents a two-photon absorption cross section of 45 GM at 720 nm but is poorly luminescent in water. A detailed solvent-dependent photophysical study indicates that this luminescence quenching is not due to the direct coordination of O−H vibrators to the metal center but to the increase of nonradiative processes in a protic solvent induced by an internal isomerization equilibrium.

INTRODUCTION

The sensitization of europium or terbium luminescence by nonlinear two-photon excitation is recently becoming a promising strategy for the design of a new generation of bioprobes for multiphoton microscopy imaging techniques.[1,2] These new probes should combine the intrinsic advantages of two-photon excitation,[3] such as 3D resolution, low-energy excitation localized in the biological window, reduced photodamage, and photobleaching, with those of lanthanide luminescence, namely, sharp emission bands with large apparent Stokes' shifts, long excited-state lifetimes, and sensitivity to the local environment.[1b,4] The proof-of-concept of the biphotonic sensitization of lanthanide luminescence by organic ligands was established in the early 2000s by Lakowicz and co-workers.[5] The two-photon absorption efficiency estimated by the measure of the two-photon cross section (σ_2) was then improved using ligands featuring charge-transfer transitions like Michler's ketone,[6] 2-(diethylanilin-4-yl)-4,6-bis(3,5-dimethylpyrazolyl)triazine,[7] or functionalized pyridinedicarboxamide.[8] Significant σ_2 values (between 100 and 300 GM) were obtained, but the poor solubility and stability of these complexes in water preclude any practical applications as bioprobes. These limitations were partially overcome by the design of tris(dipicolinate) lanthanide complexes $[Ln(DPA)_3]^{3-}$ (DPA = pyridinedicarboxylate), where the DPA ligand was functionalized by π-conjugated donor moieties decorated with hydrosolubilizing poly(ethylene glycol) (PEG) end groups (Chart 1), leading to complexes soluble enough in water so that the first two-photon scanning microscopy experiment on fixed human cancer cells could be successfully performed.[2b] Moreover, fine tuning of the π-conjugated antenna allowed us to reach very important two-photon absorption cross sections, up to 775 GM.[9] However, the stability of this class of complexes in water remains moderate, and the complexes tend to dissociate in dilute solutions (30% of dissociation in the 10^{-4}−10^{-5}

Received: February 2, 2011
Published: May 09, 2011

Chart 1. Structures of the Europium Tris(dipicolinate) Ligand, the Target Macrocyclic Ligands (L^1 and L^2), and Related Europium(III) Complexes

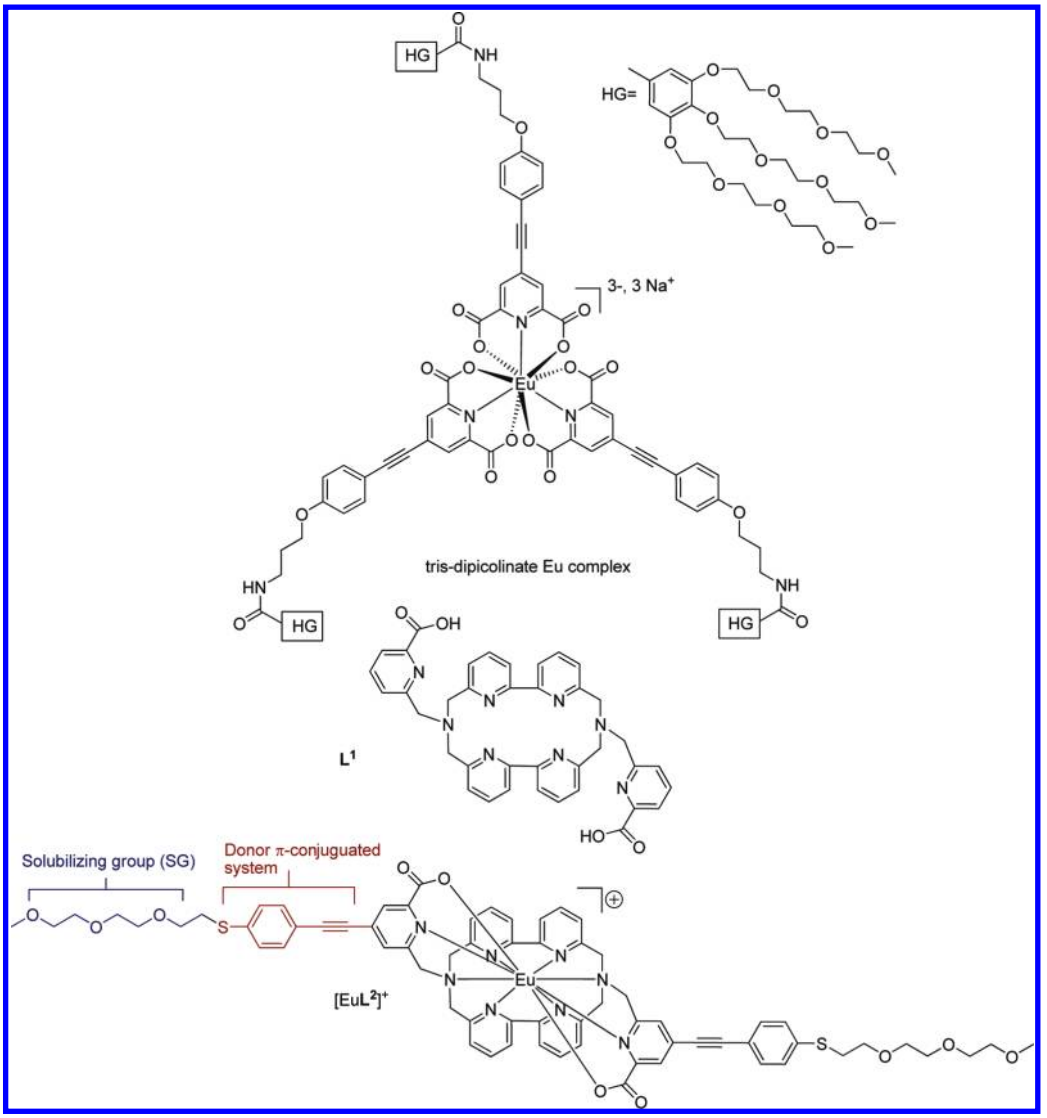

M concentration range), limiting their use in biologically relevant applications.[10,2b] In this context, we started a research project aimed at incorporating our two-photon antenna onto a macrocyclic ligand widely encountered in lanthanide coordination chemistry to improve its stability in a biological medium. Following this idea, we recently reported the functionalization of diethylenetriaminepentaacetic acid (DTPA) and DOTA macrocycles by two-photon antenna, but the nonlinear optical properties were rather modest.[11] To combine the stability and photophysical requirements, we now propose using the bis(bipyridine) azamacrocyclic platform known since the pioneering work of Lehn et al. on europium tris(bipyridine)cryptates,[12] which yields highly stable complexes presently used and commercialized in homogeneous time-resolved fluorescence bioassays and related applications.[13,14] Saturation of the coordination sphere is ensured by two additional pyridinecarboxylate pendant arms known to act as efficient chelating units,[15] which can be easily modified to behave as two-photon antenna according to the aforementioned strategy.[9,11] In this article, we report the synthesis of two new macrocyclic ligands, $\mathbf{L^{1-2}}$ (Chart 1), and their related europium(III) complexes. Whereas the nonfunctionalized $[Eu\mathbf{L^1}]^+$ complex is highly luminescent and stable in aqueous or buffer media, its functionalized counterpart $[Eu\mathbf{L^2}]^+$ retains its emission properties only in organic solvents. The surprising difference between the photophysical properties in water of these two complexes is discussed on the basis of density functional theory (DFT) calculations, solution NMR studies, and solvent-dependent photophysical measurements. Finally, the two-photon absorption properties of $[Eu\mathbf{L^2}][TFA]$ (TFA is trifluoroacetate) in organic media are presented and discussed.

RESULTS AND DISCUSSION

Synthesis. Synthesis of the pendant chelating units **4** and **11** (Scheme 1) involves a key step in the desymmeterization of the diester derivatives **2** and **7**, respectively. These monoreductions, adapted from literature procedures,[16] were successfully achieved using $NaBH_4$ (1.5 equiv) in dry methanol and scaled up to several grams. The (alkylthio)phenylethynyl fragment **9**, containing a 2-[2-(2-methoxyethoxy)ethoxy]ethyl moiety (Peg) that ensures

dx.doi.org/10.1021/ic200227b |Inorg. Chem. 2011, 50, 4987–4999

Scheme 1. Synthesis of the Chromophore Antenna Fragments

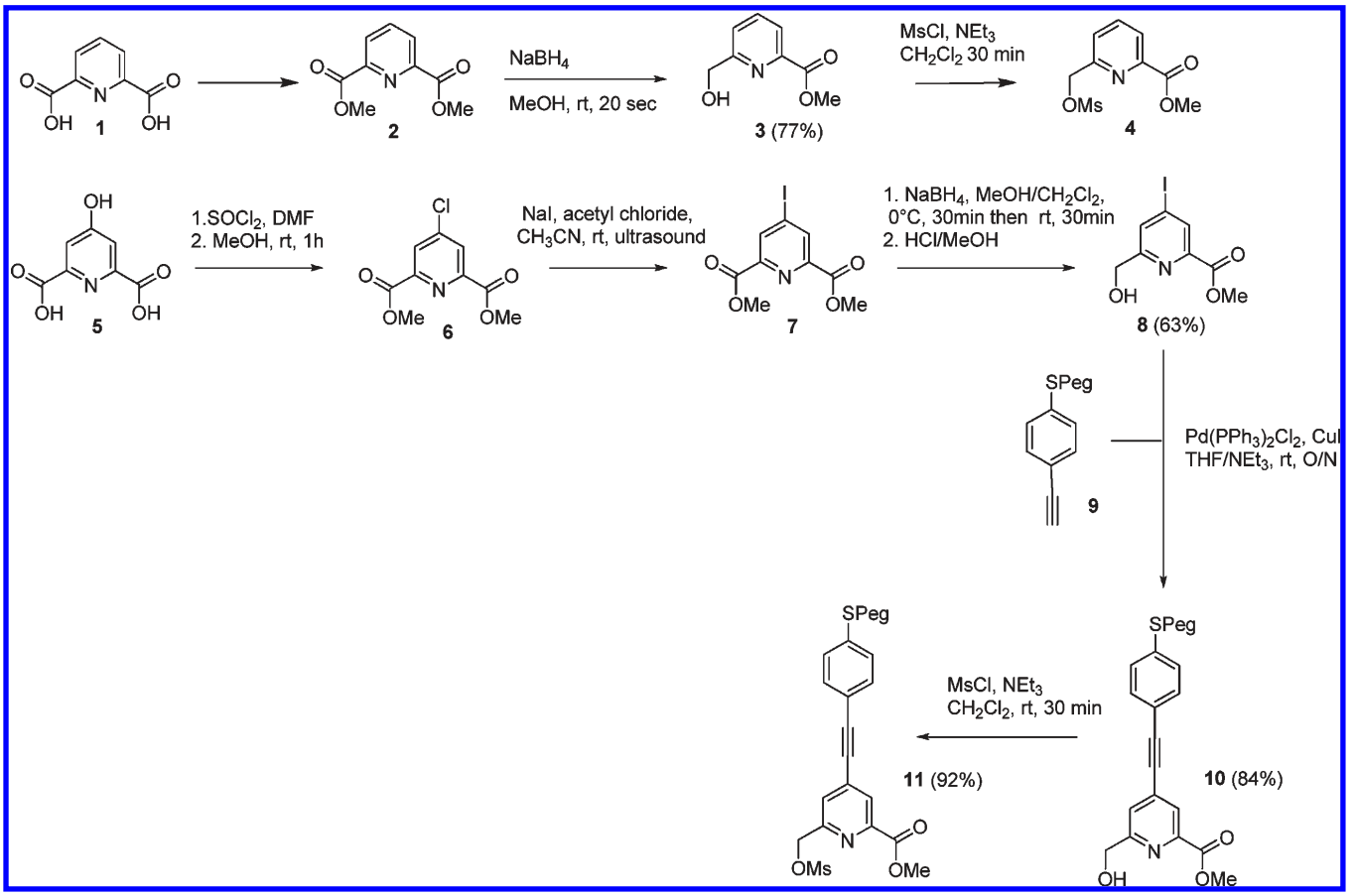

Scheme 2. Synthesis of the Ligands L^{1-2}

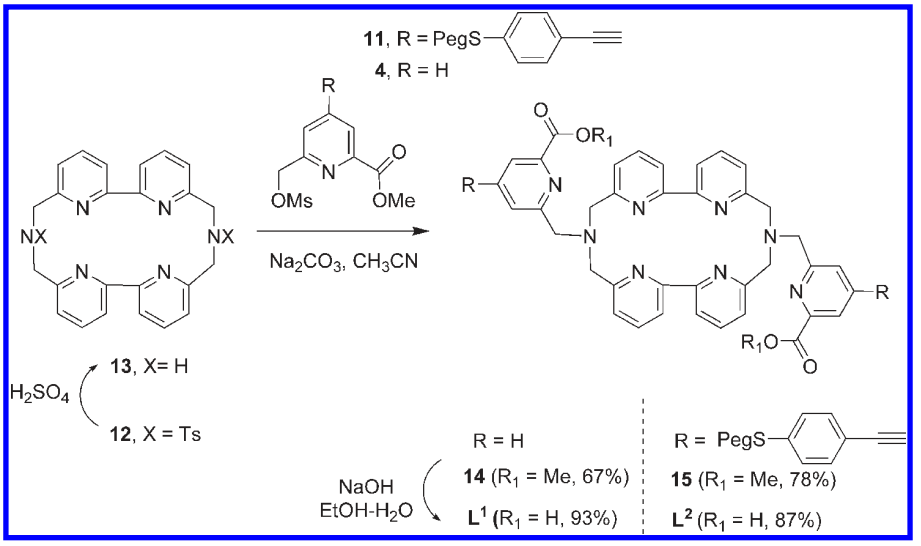

the final solubility in water, was coupled to **8** via a classical palladium-catalyzed Sonogashira cross-coupling reaction, leading to the final functionalized pendant chromophore **11** after mesylation.[11]

Synthesis of the macrocyclic ligands $\mathbf{L}^{1-2}$ was achieved in small amounts with good yield by double alkylation of the azamacrocyclic precursor **13**, featuring two nonconjugated bipyridine subunits tethered to each other via a nitrogen-containing hydrocarbon chain,[17] followed by saponification of the ester moieties in basic media (Scheme 2). The final europium complexes $[Eu\mathbf{L}^{1-2}][TFA]$ (Chart 1) were prepared in an acetonitrile solution by mixing 1 equiv of ligands $\mathbf{L}^{1-2}$ with an excess of

dx.doi.org/10.1021/ic200227b |*Inorg. Chem.* 2011, 50, 4987–4999

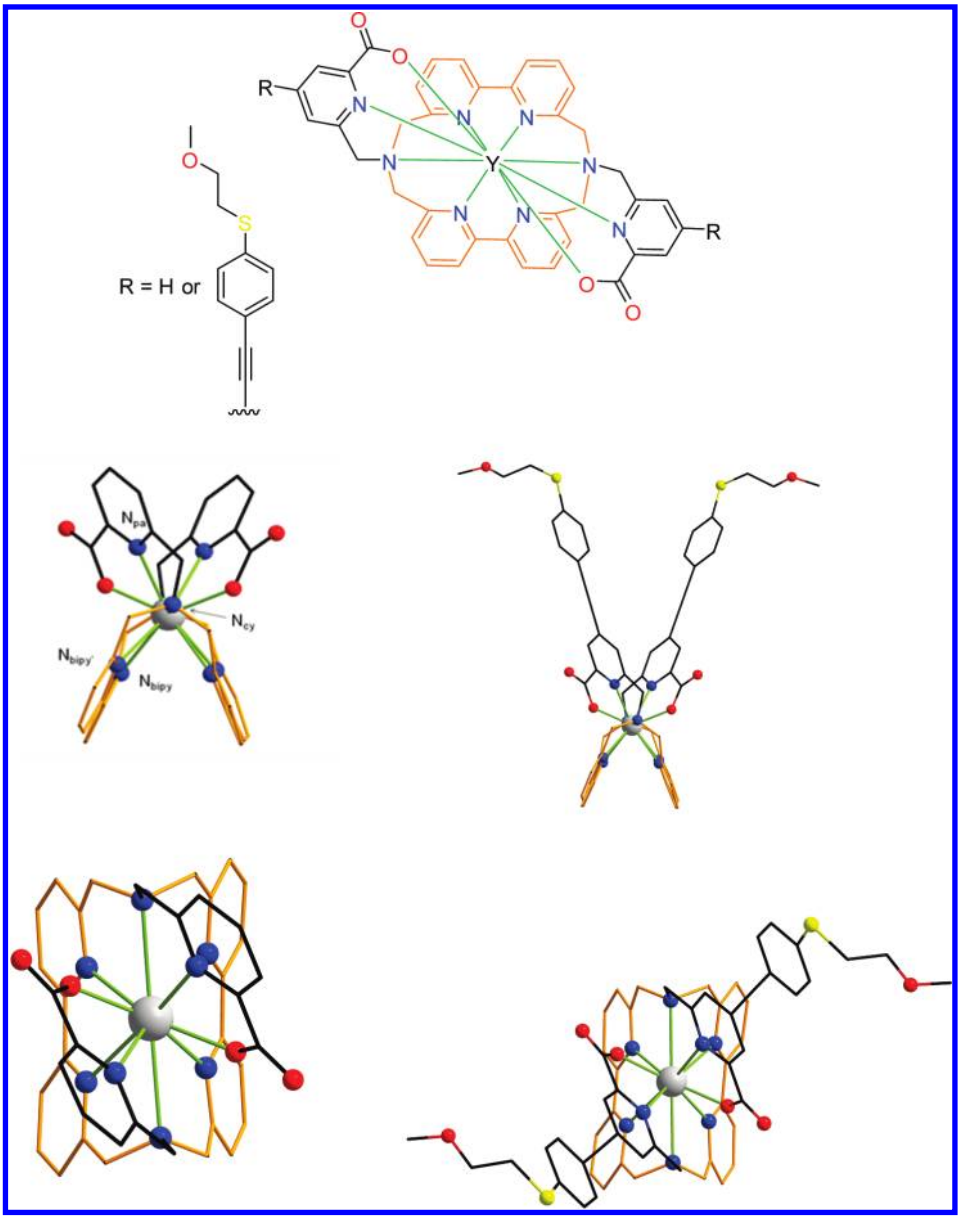

Figure 1. DFT-optimized structures of $[YL^{1}]^{+}$ (left) and $[YL^{2'}]^{+}$ (right), with the C_2 symmetry axis being vertical (up) or perpendicular to the figure (bottom). Nitrogen, oxygen, and sulfur atoms are drawn in blue, red, and yellow, respectively.

europium chloride (3 equiv) in the presence of Na_2CO_3. All syntheses were carried out on a small scale, and therefore the ligands **14**, **15**, and L^{1-2} and related complexes $[EuL^{1-2}][TFA]$ were purified, at each step, by high-performance liquid chromatography (HPLC; see the Experimental Section for details and the Supporting Information, Figure S1) and further characterized by high-resolution mass spectrometry (HRMS) analysis. In addition, the final complexes were characterized by ^{1}H NMR spectroscopy and will be detailed later. It is worth noting that a counter-ion-exchange reaction from chloride to triflate, unambiguously identified by ^{19}F NMR spectroscopy, occurs during purification of the complexes because of the presence of trifluoroacetic acid in the eluent.

DFT Geometry Optimizations. In order to interpret the spectroscopic data, DFT geometry optimizations (see the Computational Details section) were undertaken on $[ML^{1}]^{+}$ and model $[ML^{2'}]^{+}$ (M = Y, Lu) featuring a shorter thioalkyl fragment. The paramagnetic Eu^{III} ion was replaced by the diamagnetic Y^{III} or Lu^{III} ion for calculation facilities.[18] The optimized structures are represented in Figure 1 in the case of yttrium (see the Supporting Information, Figure S2, for lutetium complexes), and selected bond lengths are compiled in Table 1. The yttrium and lutetium complexes are isostructural. The only observed difference lies in the shortening of the metal-to-ligand bond lengths when Y^{III} is replaced by Lu^{III}, featuring a smaller ionic radius (Table 1). It is also worth noting that ligand functionalization by a π-conjugated chromophore has a negligible impact on the coordination polyhedron (see the comparison between $[ML^{1}]^{+}$ and $[ML^{2}]^{+}$ in Table 1). In all complexes, the central metal ion is bound to the 10 donor atoms of the ligands, among which 8 nitrogen atoms are from the bis(bipyridyl) moieties ($4N_{bipy}$), the azamacrocycle ($2N_{cy}$), and the picolinic acid pendant arm ($2N_{pa}$). The coordination sphere is completed by two oxygen atoms from the carboxylate functions. The

dx.doi.org/10.1021/ic200227b |*Inorg. Chem.* 2011, 50, 4987–4999

bis(bipyridine) azamacrocycle can be considered as a platform filling half of the coordination space with a rather small angle (60°) between the two bipyridyl fragments. The two picolinic acid pendant arms act as a scorpionate ligand lying above the macrocyclic platform in a syn-like conformation. Such types of conformations are generally encountered for related complexes based on triazacyclononane[15c,d] or crown ether[15e,f] platforms. Because of the lack of flexibility of the bis(bipyridine) azamacrocycle, each bipyridine ligand is slightly distorted with a twist angle of ca. 10°. As a consequence, the complexes present a low C_2 symmetry, where the symmetry axis is perpendicular to the pseudoplane made by the four N_{bipy} atoms (Figure 1). The lack of macrocyclic ligand flexibility combined with the rather unusual 10-coordinate structure[15f] in $[LuL^1]^+$ is also responsible for the significantly longer metal-to-ligand bond lengths.[19] As an example, the Lu−N_{bipy} bond lengths are found in the 2.6−2.7 Å range and the Lu−N_{cy} distances are even longer at about 2.84 Å. On the contrary, the more flexible pendant pyridinecarboxylate arms are more strongly coordinated with a Lu−N_{pa} bond length of around 2.55 Å in $[LuL^2]^+$ in the range of those measured for related 1,7-diaza-12-crown-4[15e] or triazacyclononane[15c] platforms (2.4−2.6 Å).

Solution Structures of [EuL$^{1-2}$][TFA] Complexes. These structures were investigated by ^{1}H NMR spectroscopy. In D_2O at room temperature, the $[EuL^1][TFA]$ complex exhibits a well-resolved spectrum, spread over 40 ppm because of the paramagnetism of europium (Figure 2). Each proton of the azamacrocycle and the benzylic protons of the pendant arms are diastereotopic, a signature of the rigidification of the macrocyclic ligand upon complexation. As a consequence, the azamacrocyclic protons, in the closer vicinity of the metal, are strongly high-field shifted (in the [−5, −20] ppm range; Figure 2) and exhibit $^2J_{gem}$ coupling constants in the range of 14.4−16.0 Hz. In addition, three different pyridinyl systems can be identified but not unambiguously assigned, which reveals that the nonequivalence of each pyridine subunit of the bipyridine moieties is preserved in solution. In marked contrast, the spectrum of $[EuL^2][TFA]$ in D_2O is only composed of broad signals at room temperature, a signature of the dynamic behavior of the complex in this solvent. On the other hand, in $CDCl_3$, the spectrum becomes well resolved (Figure 3) and the para-functionalization of the picolinic acid pendant arms allows a definitive assignment of each signal by 2D COSY experiments. These experiments unravel two sets of signals for the bipyridine fragment and the equivalence of the picolinic acid moieties. It is worth noting that two NMR signals belonging to one pyridine of the bipyridine ligand are merged at 6.3 ppm. This observation is unambiguously confirmed thanks to variable-temperature measurements: because of the temperature dependence of the paramagnetic chemical shift, these two signals are well resolved by increasing the temperature to 40 °C. Therefore, the C_2 symmetry of both complexes observed in the optimized geometries is confirmed in solution by ^{1}H NMR.

Table 1. Selected Bond Lengths (Å) of the DFT-Optimized Complexes $[ML^1]^+$ and $[ML^{2'}]^+$

distance (Å)	$[YL^1]^+$	$[YL^{2'}]^+$	$[LuL^1]^+$	$[LuL^{2'}]^+$
M−N_{bipy}	2.658	2.703	2.663	2.670
M−$N_{bipy'}$	2.700	2.659	2.615	2.621
M−N_{pa}	2.614	2.589	2.578	2.551
M−N_{cy}	2.834	2.833	2.844	2.843
M−O	2.279	2.282	2.216	2.219

Photophysical Properties of Europium Complexes. The absorption and emission properties of the two complexes were investigated in water and in phosphate or HEPES buffers. $[EuL^1][TFA]$ presents absorption bands localized in the UV region with a modest extinction coefficient (λ_{max} = 308 nm, ε_{max} = 18 000 M^{-1} cm^{-1}) that are classically observed for $\pi-\pi^*$ transitions of pyridinic/picolinic ligands (Figure 4). As expected,

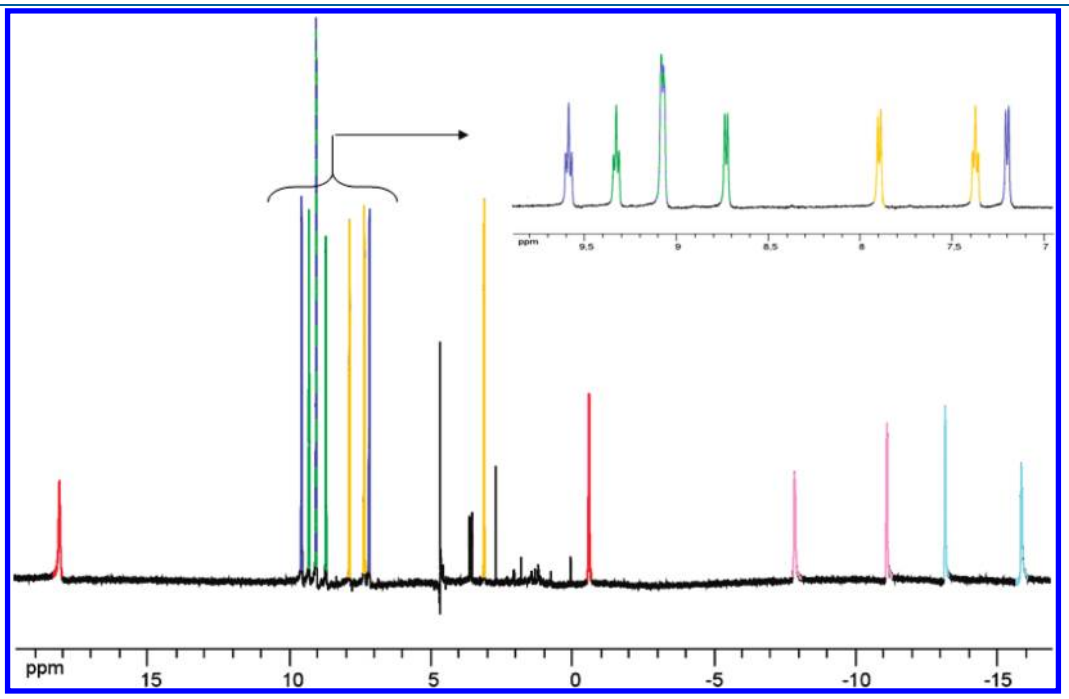

Figure 2. ^{1}H NMR (500 MHz, 20 °C) spectrum of $[EuL^1][TFA]$ in D_2O with magnification of the aromatic region. The aliphatic protons are indicated in red, pink, and cyan, whereas the pyridinyl ones are in blue, green, and yellow.

dx.doi.org/10.1021/ic200227b |*Inorg. Chem.* 2011, 50, 4987–4999

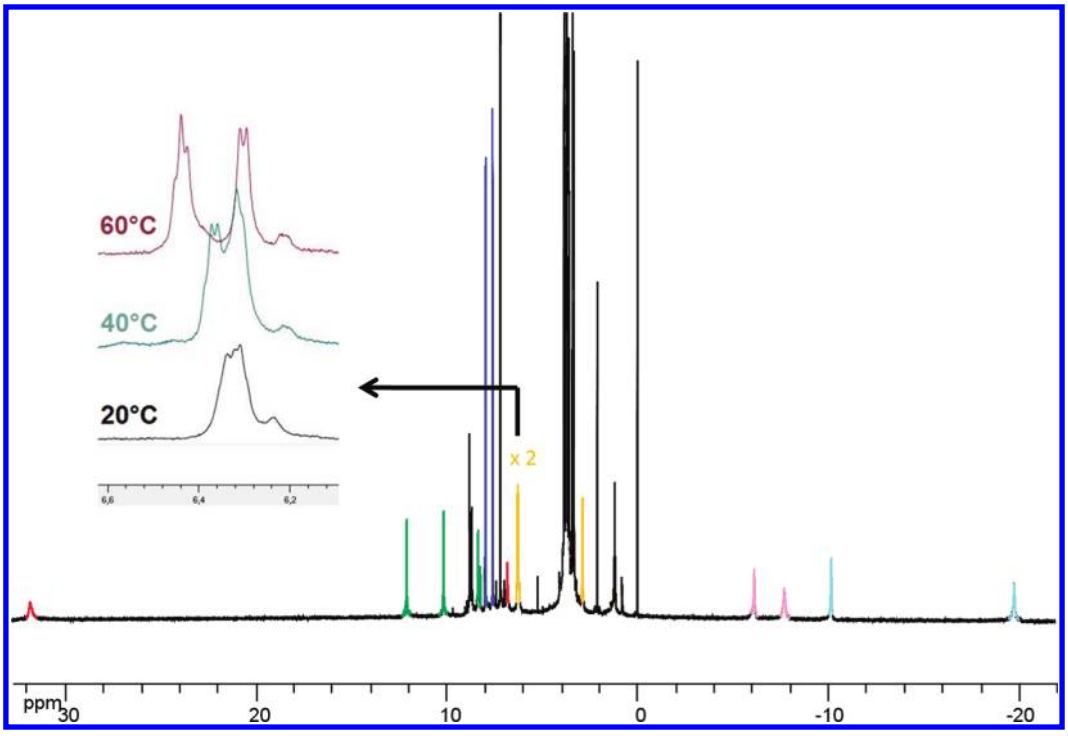

Figure 3. ^{1}H NMR (500 MHz, 20 °C) spectrum of [Eu**L**^{2}][TFA] in $CDCl_3$. The inset displays a portion of the variable-temperature ^{1}H NMR spectrum illustrating the fusion of two signals in one broad peak. The aliphatic protons are indicated in red, pink, and cyan, whereas the pyridinyl ones are in blue, green, and yellow.

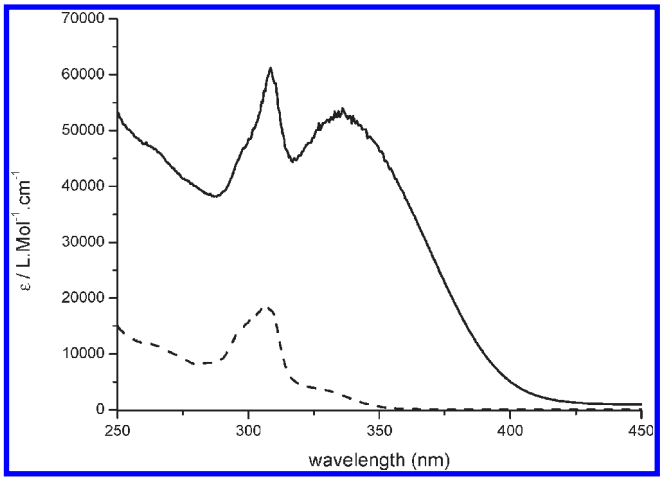

Figure 4. Absorption spectra of [Eu**L**^{1}][TFA] (dashed line) and [Eu**L**^{2}][TFA] (solid line) in water.

the introduction of donor-functionalized π-conjugated moieties in [Eu**L**^{2}][TFA] results in the appearance of an additional broad intense transition (λ_{max} = 337 nm, ε_{max} = 53 000 M^{-1} cm^{-1}) assigned to an intraligand charge-transfer (ILCT) transition from the thioalkyl electron-donating group to the picolinic electron-accepting fragment,[20] in addition to the 308 nm feature ($\varepsilon_{max} \approx$ 61 000 M^{-1} cm^{-1}). It is now well established that such ILCT transitions are necessary to ensure efficient two-photon absorption by the complex[6−9] and are further able to induce an efficient europium sensitization via an alternative "ILCT sensitization pathway".[1b,20,21]

Excitation in the $\pi-\pi^*$ transitions of [Eu**L**^{1}][TFA] results in bright-red europium luminescence with a reasonable 0.13 luminescence quantum yield efficiency and a long luminescence lifetime (1.8 ms) in water. The same lifetimes and quantum yields were obtained in HEPES or phosphate buffer solutions. It is also worth noting that the introduction of potassium fluoride in the solution mixture has no effect on the luminescence properties indicating that the coordination sphere of the central metal ion is fully saturated by the macrocyclic ligand. In addition, the luminescence lifetime remains constant upon dilution of the complex from 10^{-5} up to 10^{-7} M or when further diluted to 6 nM in HEPES and phosphate buffers including 0.1% bovine serum albumin (BSA), which is under experimental conditions appropriate for bioassays. Moreover, upon the addition of 20 mM EDTA to this solution, no loss of luminescence was observed, underlining that, under these experimental conditions, no dissociation occurs. These results confirm the NMR observations and clearly establish that the introduction of pyridinecarboxylate pendant arms strongly stabilizes the [Eu**L**^{1}][TFA] complex in water compared to analogous chelates featuring bipyridine or phenanthroline pendant arms.[22] The [Eu**L**^{1}][TFA] emission spectrum is very well resolved (Figure 5, top) and shows the bands corresponding to the $^{5}D_0 \rightarrow {}^{7}F_J$ (J = 0−4) transitions. The splitting of these transitions and their relative intensities are the signature of the ligand-field effect and are directly related to the symmetry of the coordination polyhedron. In the present case, the observed splitting of the J = 2 transition in several bands is a signature of a low-symmetry complex, but resolution of the spectrum recorded in water is not sufficient to draw any definitive conclusion (vide infra).

In marked contrast, the emission of the functionalized analogue [Eu**L**^{2}][TFA] is very weak in aqueous media, as is illustrated by the low luminescence quantum yield (<0.02), the shorter luminescence lifetime, and the less resolved spectrum with

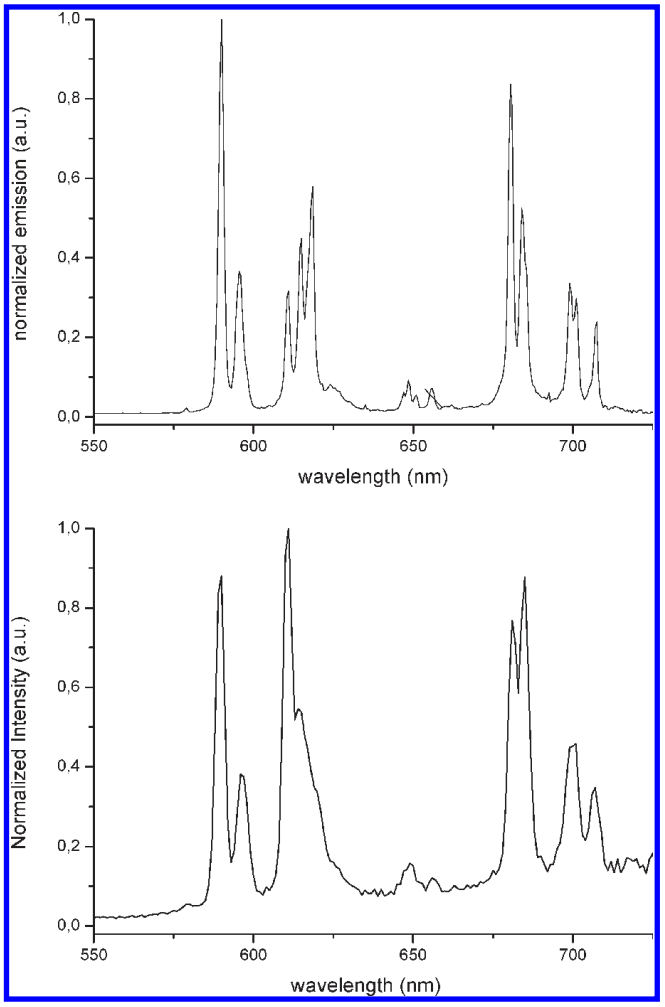

Figure 5. Normalized luminescence spectra of [Eu**L**^{1}][TFA] (top) and [Eu**L**^{2}][TFA] (bottom) in a phosphate buffer (pH = 7; λ_{ex} = 330 nm). The small peak at 660 nm corresponds to the excitation wavelength harmonic.

Table 2. Photophysical Data of [EuL^{1-2}][TFA] (ca. 10^{-6} M) in Water at Room Temperature

	[Eu**L**^{1}][TFA]		[Eu**L**^{2}][TFA]	
solvent	ϕ_{Eu}	τ_{obs} (ms)	ϕ_{Eu}	τ_{obs} (ms)
H_2O	0.13	1.80	0.013	0.53
D_2O	[a]	[a]	0.017	0.65

[a] Not measured.

broader emission bands (Table 2 and Figure 5). This emission quenching cannot be simply attributed to coordination of the water molecules because the lifetime in D_2O (0.65 ms) is close to that in H_2O (0.53 ms) (Table 2). The hydration number q_{corr} can be estimated as ca. 0.04 on the basis of Horrocks' phenomenological hydration second equation, taking into account the correction factor describing the outer-sphere water molecule contribution,[23] $q_{corr} = A'(\Delta k - \alpha)$ with A' = 1.11 ms for Eu^{III}, $\Delta k = 1/\tau_{obs}(H_2O) - 1/\tau_{obs}(D_2O)$, and α = 0.31 ms^{-1}. This result suggests that no water molecule is directly bonded to the metal center, with the lifetime variation being mainly due to second or outer-sphere water molecules. In order to gain deeper insight into the differences observed between [Eu**L**^{1}][TFA] and [Eu**L**^{2}][TFA], an extensive study of the influence of the solvent on the photophysical properties of [Eu**L**^{2}][TFA] was undertaken.

Table 3. Calculated Values of τ_r, k_r, Σk_{nr}, η_{Eu}, and η_{sens} for [EuL^2][TFA] (ca. 10^{-6} M) in Various Solvents and [EuL^1][TFA] (ca. 10^{-6} M) in Water Using the Room Temperature Experimentally Determined Quantities ϕ_{Eu}, τ_{obs}, and $[I(0,1)/I_{tot}]$

solvent	ϕ_{Eu}[a]	τ_{obs}[b] (ms)	τ_r (ms)	η_{Eu}	η_{sens}	$[I(0,1)/I_{tot}]$	k_r/ 10^2 s^{-1}	Σk_{nr}/ 10^2 s^{-1}
			[Eu**L**^{2}][TFA]					
DCM	0.11	1.24	4.24	0.29	0.38	0.17	2.3	5.7
MeCN	0.17	2.66	5.15	0.52	0.33	0.17	1.9	1.8
DMSO	0.10	1.88	4.18	0.45	0.22	0.18	2.4	2.9
MeOH	0.008	0.80	5.40	0.15	0.05	0.17	1.8	10.7
EtOH	0.025	0.81	5.23	0.15	0.16	0.18	1.9	10.4
H_2O	0.013	0.53	6.84	0.08	0.02	0.22	1.5	17.2
			[Eu**L**^{1}][TFA]					
H_2O	0.13	1.80	7.42	0.24	0.53	0.24	1.3	4.2

[a] λ_{ex} = 360 nm. [b] λ_{ex} = 370 nm.

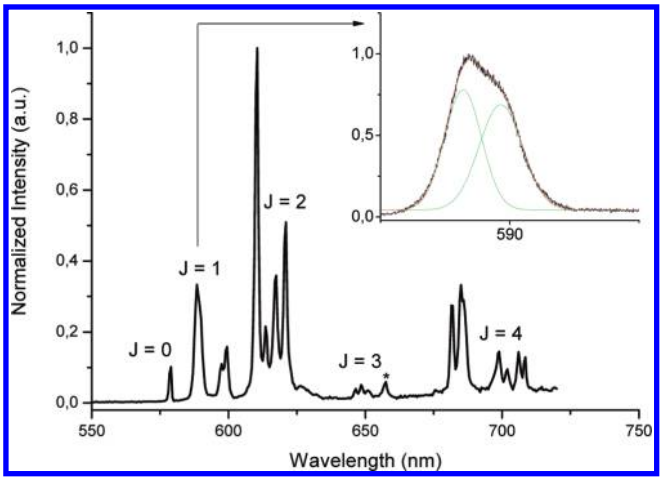

Figure 6. Emission spectrum of [Eu**L**^{2}][TFA] in DCM at room temperature (λ_{ex} = 330 nm). Inset: magnification of the first component of the $^5D_0 \rightarrow {}^7F_1$ transition and fit using Gaussian functions (green curves; sum in red).

Structural Information Probed by Luminescence Measurements. Owing to the presence of the Peg functionalization, [Eu**L**^{2}][TFA] is very soluble in most organic solvents like dichloromethane (DCM), acetonitrile (MeCN), dimethyl sulfoxide (DMSO), methanol (MeOH), or ethanol (EtOH) and slightly soluble in methyltetrahydrofuran (MeTHF). In all solvents, very well-resolved emission spectra characteristic of an Eu^{III}-centered emission were recorded. The respective luminescence quantum yields and lifetimes are compiled in Table 3. Figure 6 illustrates a representative emission spectrum recorded using a 0.3-nm resolution, the highest afforded by our experimental setup. Excitation in the antenna broad absorption band at 330 nm gives an emission spectrum featuring the $^5D_0 \rightarrow {}^7F_J$ transitions (J = 0−4) characteristic of Eu^{III}, with 0.1, 1, 2.7, 0.2, and 2.0 relative corrected intensity patterns, signature of a low-symmetry

dx.doi.org/10.1021/ic200227b |*Inorg. Chem.* 2011, 50, 4987–4999

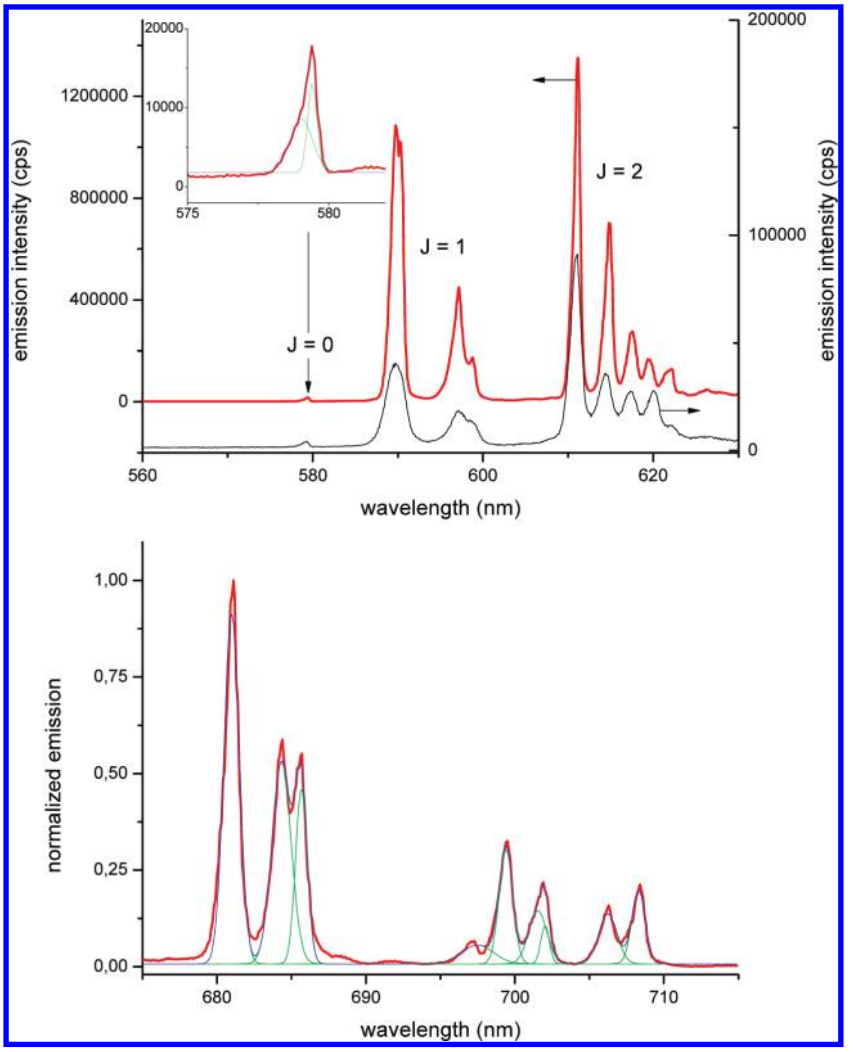

Figure 7. (Top) Emission spectra of [Eu$\mathbf{L}^2$][TFA] in MeOH/EtOH (1/4, v/v) at room temperature (black curve) and in frozen glass at 77 K (red curve) using λ_{ex} = 330 nm. Inset: magnification on the $^5D_0 \rightarrow {}^7F_0$ transition and fit using Gaussian functions (green curves; sum in red). (Bottom) Magnification of the J = 4 transition and decomposition into nine Gaussian curves (green curves; sum in blue).

environment of the emitting center. In addition, in the case of europium, the splitting of each $^5D_0 \rightarrow {}^7F_J$ transition is correlated to ligand- (crystal-)field effects and is therefore representative of the local symmetry. For a C_2 compound, as anticipated for the [Eu$\mathbf{L}^2$][TFA] complex according to DFT and NMR data, a splitting of each transition in $2J + 1$ sublevels is predicted by theory,[24] in line with experimental data.[25] In the present case, whereas the J = 1 transition is split into three main sublevels, its first component (Figure 6, inset) is clearly the sum of two individual transitions and the resulting global splitting is then larger than the prediction. In order to obtain a better resolution, low-temperature emission spectra (77 K) were recorded in EtOH/MeOH (1/4, v/v) frozen organic glasses.[26] Lowering the temperature results in a ca. 10 times enhancement of the emission intensity, as illustrated by the relative areas of the room temperature and 77 K spectra (Figure 7, top), accompanied by a large increase of the lifetime from 0.85 ms at room temperature up to 2.4 ms at 77 K. Indeed, the vibronic broadening of the transition is strongly reduced and the full width at half-maximum (fwhm) of the hypersensitive J = 2 transition decreases from 42 cm^{-1} at room temperature to 25 cm^{-1} at 77 K, leading to enhanced resolution. The J = 2 transition is now clearly split into five sublevels, and the transition to the J = 4 level exhibits nine sublevels after decomposition into Gaussian components (Figure 7, bottom), as is expected for a C_2-symmetric complex. Furthermore, the J = 1 transition is clearly composed of three main components, but the first one appears as a doublet. The explanation of this doublet can be found in a careful examination of the J = 0 transition (inset of Figure 7, top): this band cannot be satisfactorily fitted by a single Gaussian and is better described as the sum of two contributions. This result suggests the presence of two emitting species at low temperature, both presenting very similar local environments with overall C_2 symmetry, with the only observable emission difference being the presence of a doublet in the first component of the J = 1 transition. These two species may originate from an internal isomerization dynamic equilibrium between a 10-coordinated species [Eu10-$\mathbf{L}^2$]$^+$ and a nine-coordinated isomer [Eu9-$\mathbf{L}^2$]$^+$ in which the longest Eu−N_{cy} bond is broken (Figure 8). This dynamic equilibrium could be assisted by additional exocyclic hydrogen-bond formation between a protic solvent (water, D_2O, alcohols, etc.) and the uncoordinated nitrogen lone pair. This dynamic equilibrium is

dx.doi.org/10.1021/ic200227b |*Inorg. Chem.* 2011, 50, 4987–4999

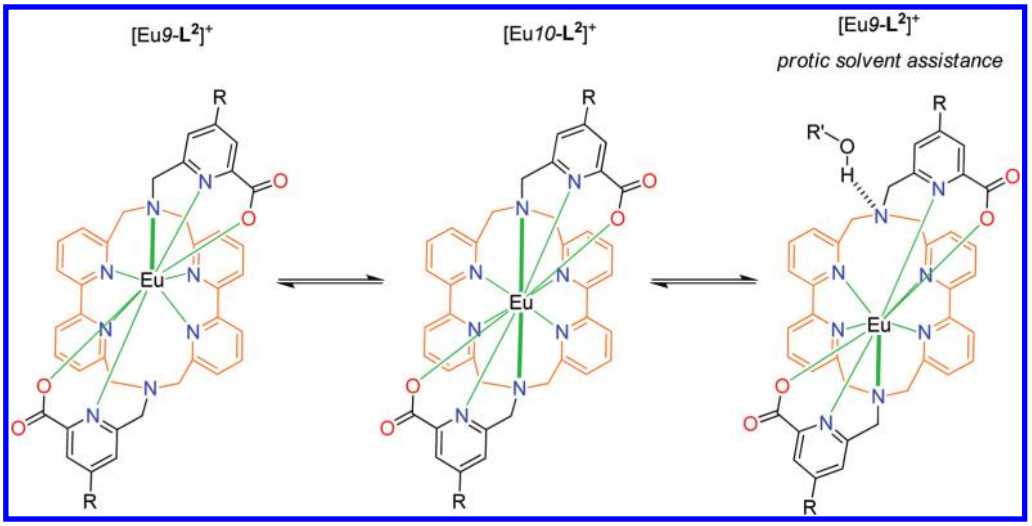

Figure 8. Hypothesis for the internal isomerization dynamic equilibrium.

too fast to be observed by ^{1}H NMR at low temperature in aprotic $CDCl_3$. On the other hand, in protic solvents like D_2O, $[EuL^2]^+$ presents only broad ^{1}H NMR signals similar to those observed in the case of coalescence.[27]

Solvent Dependence of the Photophysical Properties. In order to gain deeper insight into these solvent effects, the relevant radiative and nonradiative parameters were deduced from experimental data (spectra, quantum yields, and lifetimes) according to the works of Werts et al.[28] and Beeby et al.[29] Using this method, the overall europium quantum yield of luminescence (ϕ_{Eu}) is defined as the product of the efficiency of sensitization (η_{sens}, i.e., here the fraction of energy transferred from the donor state to the Eu^{III} accepting levels) and the quantum efficiency of the metal-centered luminescence upon direct excitation into the f levels (η_{Eu}).

$$\varphi_{Eu} = \eta_{sens}\eta_{Eu}$$

In this equation, $\eta_{Eu} = \tau_{obs}/\tau_r$, where τ_{obs} represents the experimental luminescence lifetime of the complex and τ_r, the pure radiative lifetime, calculated from $k_r = 1/\tau_r = A(0,1)[I_{tot}/I(0,1)]$. The constant $A(0,1)$ is the spontaneous emission probability of the $^5D_0 \rightarrow {}^7F_1$ transition, equal to 39.4 s^{-1} in DCM, and $I_{tot}/I(0,1)$ is the ratio of the total integrated emission intensity to the intensity of the $^5D_0 \rightarrow {}^7F_1$ transition. Finally, Σk_{nr} can be deduced knowing k_r and τ_{obs}, from the relationship $\Sigma k_{nr} = 1/\tau_{obs} - 1/\tau_r$. This procedure was applied to $[EuL^2][TFA]$ in various solvents and to $[EuL^1][TFA]$ in water. All data are summarized in Table 3.[30] In all organic solvents, the symmetries of the complexes appear to be identical, as inferred from almost constant $[I(0,1)/I_{tot}]$ ratios (0.17−0.18); henceforth, almost negligible variations in the radiative lifetime (τ_r) or radiative constant rate (k_r) are observed. In protic solvents (water and alcohol), a strong decrease in the luminescence lifetime induces a drop in η_{Eu}, which decreases to 0.08−0.15 compared to that in aprotic solvents of various polarity (DCM, MeCN, DMSO, etc.), where η_{Eu} is in the range of 0.29−0.52. As a consequence, the nonradiative decay rates (Σk_{nr}) are far larger in protic solvents. These observations explain the important decrease of the luminescence quantum yield efficiency in protic solvents (Table 3) with, for example, a drop from 0.17 in MeCN to less than 0.01 in MeOH. Interestingly, this decrease is not, as is usually observed, due to the direct coordination of O−H vibrators to the europium emitting ion but to the dramatic increase of alternative nonradiative deactivation processes like the above-mentioned internal isomerization equilibrium between $[Eu10\text{-}L^2]^+$ and $[Eu9\text{-}L^2]^+$. Other potential contributions could also come from proximate high-energy O−H vibrators located in the outer coordination sphere.[23b] As a consequence, lowering the temperature to 77 K slows the dynamic equilibrium kinetics, resulting in reduced contributions of the related nonradiative processes and, hence, in the recovery of the luminescence intensity (Figure 7, top). Finally, applying the same procedure to $[EuL^1][TFA]$ in water (Table 3) clearly indicates that the nonradiative rates (Σk_{nr}) in water are far smaller than those for the functionalized counterpart (420 vs 1723 s^{-1}). This result indicates that the internal isomerization equilibrium does not occur for $[EuL^1][TFA]$, which explains the enhanced luminescence quantum yield of this compound in water. Finally, both NMR and luminescence experiments unambiguously demonstrate that the lateral donor π-conjugated functionalization in $[EuL^2][TFA]$ induces more lability in the complex, which therefore presents a more pronounced binding exchange dynamic behavior, i.e., the internal isomerization equilibrium in protic solvents. The electronic reasons behind this difference are not well understood and are currently under investigation in our group.

Two-Photon Absorption Properties. The two-photon absorption properties of $[EuL^2][TFA]$ featuring a π-conjugated antenna were studied in a DCM solution by monitoring the two-photon excited luminescence in the 700−900 nm spectral range. Coumarin-307 was used as the standard, according to the experimental protocol described by Xu and Webb,[31] and excitation was achieved with a femtosecond Ti:sapphire pulsed laser. The two-photon excitation spectrum (Figure 9) matches the wavelength-doubled single-photon one. This result indicates that transitions to the lowest-energy excited state, namely, a charge-transfer state (ILCT), are one- and two-photon-allowed, in agreement with the symmetry of the complex and with the two-photon selection rules in the case of noncentrosymmetric derivatives. At 720 nm, $[EuL^2][TFA]$ presents a two-photon cross section of 45 GM. It is worth noting that the maximal absorption wavelength is located out of our laser excitation range and that only the red tail of the two-photon absorption spectrum

dx.doi.org/10.1021/ic200227b |Inorg. Chem. 2011, 50, 4987–4999

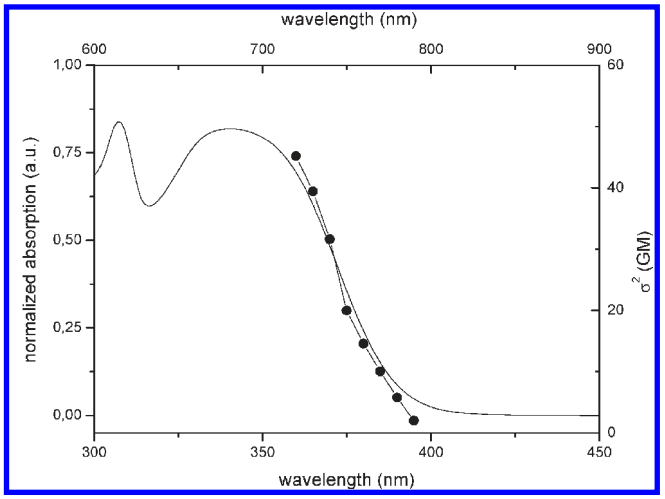

Figure 9. Two-photon excitation spectrum of [Eu$\mathbf{L}^2$][TFA] in a DCM solution (●, upper abscissa). Superimposed on this plot is the single-photon absorption spectrum (—, lower abscissa).

was measured. These two-photon photophysical properties are very similar to those observed for the tris(dipicolinate)europium complex, featuring a similar π-conjugated donor antenna with a σ_2 value of 53 GM at 700 nm.[9]

■ CONCLUSION

A new europium-based chelate system has been designed, aiming to combine high thermodynamic stability in water with efficient two-photon absorption and luminescence properties, two aspects that are essential for an optical bioprobe. To that end, two new bis(bipyridine) azamacrocylic ligands featuring or not π-conjugated donor picolinic pendant arms were prepared. The nonfunctionalized ligand leads to the formation of a highly water-stable europium complex featuring bright luminescence properties but a poor two-photon absorption cross section. On the other hand, the europium complex with the ligand based on the extended conjugated antenna presents a two-photon absorption cross section of 45 GM at 720 nm but is not very luminescent in water. A detailed photophysical study conducted in various solvents indicates that this luminescence quenching is not due to the direct coordination of O−H vibrators to the metal center but to the increase of nonradiative processes in a protic solvent induced, in part, by an internal isomerization equilibrium. It appears that π-electron-donating functionalization has a negative influence on the complex dynamics. This effect is presently not fully understood and will have to be overcome in the design of opti-
mized lanthanide-based bioprobes for two-photon scanning laser microscopy imaging.

■ EXPERIMENTAL SECTION

General Procedures. NMR spectra (^{1}H and ^{13}C) were recorded at room temperature on a Bruker AC 200 spectrometer operating at 200.13 and 50.32 MHz for ^{1}H and ^{13}C, respectively, and on a Bruker Advance spectrometer operating at 500.10 and 125.75 MHz for ^{1}H and ^{13}C, respectively. Data are listed in parts per million (ppm) and are reported relative to tetramethylsilane (^{1}H and ^{13}C); residual solvent peaks of the deuterated solvents were used as internal standards. UV/vis absorption measurements were recorded on a Jasco V670 absorption spectrometer. Low-resolution mass spectrometry was carried out on a Agilent 1100 series LC/MSD apparatus. The compounds (**14** and **15**), ligands ($\mathbf{L}^1$ and $\mathbf{L}^2$), and related europium complexes ([Eu($\mathbf{L}^1$)][TFA] and [Eu($\mathbf{L}^2$)][TFA]) were analyzed by reversed-phase HPLC (RP-HPLC) using a Waters Alliance 2695 system coupled with Waters 996 photodiode array detector and a Micromass ZQ Waters 2000 mass spectrometer. The procedure developed was 0.1% formic acid in water/MeCN as the mobile phase using a XBridge C18, 3.5 μm, 4.6 × 100 mm as the column. Purifications have been carried out using preparative RP-HPLC Shimadzu LC-8A and XBridge C18, OBD, 19 × 100 mm as the column with 0.1% TFA in 95% water/MeCN isocratic flow as the mobile phase. HRMS was performed using a Bruker MicroTOF-Q II apparatus (precision 1−5 ppm) equipped with an electrospray source using highly diluted samples in a MeOH/CDM/water/formic acid mixture (46.1:38.4:15.4:0.1, v/v). The experimental sequences for the preparation of compounds **4**,[16] **7**,[32] **9**,[9] and **13**[17] were reproduced from literature data.

Computational Details. DFT geometry optimizations with no symmetry constraint were carried out with the *Gaussian 03* (revision D.01) package,[33] employing the hybrid functional PBE0.[34] The "Stuttgart/Dresden" basis sets and effective core potentials were used to describe lanthanide atoms,[35] whereas all other atoms were described with the D95 basis sets.[36]

Luminescence. Emission spectra were measured using a Horiba-Jobin-Yvon Fluorolog-3 spectrofluorimeter, equipped with three-slit double-grating excitation and emission monochromators with dispersions of 2.1 nm/mm (1200 grooves/mm). The steady-state luminescence was excited by unpolarized light from a 450 W continuous-wave xenon lamp and detected at an angle of 90° for diluted solution measurements (10 mm quartz cell) by a red-sensitive Hamamatsu R928 photomultiplier tube. Spectra were reference-corrected for both the excitation source light-intensity variation (lamp and grating) and the emission spectral response (detector and grating). Phosphorescence lifetimes (>30 μs) were obtained by pulsed excitation using a FL-1040 UP xenon lamp. Luminescence decay curves were fitted by least-squares analysis using *Origin*. Luminescence quantum yields Q were measured in a diluted water solution with an absorbance lower than 0.1 using the equation $Q_x/Q_r = [A_r(\lambda)/A_x(\lambda)][n_x^2/n_r^2][D_x/D_r]$, where A is the absorbance at the excitation wavelength (λ), n the refractive index, and D the integrated luminescence intensity. "r" and "x" stand for the reference and sample. Here, the reference is quininebisulfate in a 1 N aqueous sulfuric acid solution (Q_r = 0.546). Excitation of the reference and sample compounds was performed at the same wavelength.

Lifetime measurements at low concentrations (6−10 nM) were performed in 0.1 M phosphate (pH 7) or 0.05 M HEPES (pH 7) with or without 0.4 M KF. All buffers contained 0.1% BSA. The solutions were distributed in Costar 96 black well flat bottom plates, and luminescence decay was measured on a Rubystar (BMG labtech) plate reader at 620 nm (exc 337 nm) using the "advanced mode" option.

Two-Photon Excited Luminescence Measurements. The TPA cross-sectional spectrum was obtained by up-conversion luminescence using a Ti:sapphire femtosecond laser in the range of 700−900 nm. The excitation beam (5 mm diameter) is focalized with a lens (focal length 10 cm) at the middle of the 10-mm cell. Emitted light was collected at 90° and was focused into an optical fiber (600 μm diameter) connected to an Ocean Optics S2000 spectrometer. The incident beam intensity was adjusted to 50 mW in order to ensure an intensity-squared dependence of the luminescence over the whole spectral range. The detector integration time was fixed to 1 s. Calibration of the spectra was performed by comparison with the published 700−900 nm Coumarin-307 two-photon absorption spectrum[31] (quantum yield = 0.56 in EtOH). The measurements were done at room temperature in DCM and at a concentration of 10^{-4} M.

Synthesis. *Compound* ***8***. To a suspension of dimethyl 4-iodopyridine-2,6-dicarboxylate (7; 2 g, 6.23 mmol) in MeOH (40 mL) cooled at

dx.doi.org/10.1021/ic200227b |*Inorg. Chem.* 2011, 50, 4987–4999

0 °C was added in one portion of $NaBH_4$ (473 mg, 12.5 mmol). The mixture was stirred at 0 °C for 30 min and left to reach room temperature over 30 min. The mixture was quenched by the addition of a 10% HCl solution (10 mL). The volatile components were evaporated under vacuum, and the aqueous solution was extracted with EtOAc (3 × 100 mL). The organic phases were combined, dried over Na_2SO_4, filtered, and concentrated in vacuo. The crude material was purified by flash chromatography on silica (98:2 CH_2Cl_2/MeOH) to afford the desired product as a white crystalline powder (1.15 g, 63%). ^{1}H NMR (200.13 MHz, $CDCl_3$): δ 8.37 (s, 1H), 7.95 (s, 1H), 4.81 (d, J = 4.9 Hz, 2H), 3.99 (s, 3 H), 3.09 (t, J = 4.9 Hz, 1H). ^{13}C NMR (50.33 MHz, $CDCl_3$): δ 164.4, 161.4, 147.2, 133.2, 132.9, 106.8, 64.2, 53.2. LRMS: m/z 294 ($[M + H]^+$), 316 ($[M + Na]^+$).

Compound ***10***. To a degassed solution of **8** (0.865 g, 2.95 mmol) in THF (20 mL) and **9** (0.858 g, 3.25 mmol) in Et_3N (10 mL) was added CuI (0.112 g, 0.59 mmol) and $Pd(PPh_3)_2Cl_2$ (0.207 g, 0.29 mmol). The dark-brown mixture was heated in the dark at 40 °C for 20 h. After cooling to room temperature, the black suspension was filtered and triturated with Et_2O (2 × 40 mL). The filtrate was washed with saturated aqueous NH_4Cl (2 × 50 mL) and brine (50 mL). The organic layer was dried over Na_2SO_4, filtered, and concentrated in vacuo. The crude material was purified by flash chromatography (49:1 CH_2Cl_2/MeOH), yielding a light-yellow oil (1.267 g, 84%). ^{1}H NMR (200.13 MHz, $CDCl_3$): δ 7.90 (d, J = 1.2 Hz, 1H), 7.56 (d, J = 1.2 Hz, 1H), 7.30 (d, J = 8.5 Hz, 2H), 7.17 (d, J = 8.5 Hz, 2H), 4.75 (d, J = 4.4 Hz, 2H), 4.29 (t, J = 4.4 Hz, 1H), 3.84 (s, 3H), 3.61−3.38 (m, 10H), 3.24 (s, 3H), 3.04 (t, J = 6.8 Hz, 2H). ^{13}C NMR (50.33 MHz, $CDCl_3$): δ 165.1, 161.5, 147.0, 139.2, 133.3, 132.2, 127.6, 125.4, 125.3, 118.5, 95.0, 86.6, 71.8, 70.51, 70.47, 70.40, 69.6, 64.6, 58.9, 52.9, 32.1. LRMS: = m/z 446 ($[M + H]^+$), 468 ($[M + Na]^+$).

Compound ***11***. To a solution of **10** (1.10 g, 2.56 mmol) and Et_3N (0.777 g, 7.68 mmol) in CH_2Cl_2 (100 mL) was added dropwise methanesulfonyl chloride (0.440 g, 3.84 mmol). After 30 min, the reaction was quenched by the addition of a saturated $NaHCO_3$ solution (100 mL). The organic phase was separated, dried over Na_2SO_4, filtered, and concentrated in vacuo. The crude material was purified by flash chromatography on silica (97:3 CH_2Cl_2/MeOB.L.GH) to afford the product as a bright-yellow oil (1.19 g, 92%). ^{1}H NMR (200.13 MHz, $CDCl_3$): δ 8.04 (d, J = 1.2 Hz, 1H), 7.62 (d, J = 1.2 Hz, 1H), 7.37 (d, J = 8.5 Hz, 2H), 7.22 (d, J = 8.5 Hz, 2H), 5.32 (s, 2H), 3.91 (s, 3H), 3.66−3.42 (m, 10H), 3.28 (s, 3H), 3.13−3.04 (m, 5H). ^{13}C NMR (50.33 MHz, $CDCl_3$): δ 164.7, 154.7, 147.9, 139.6, 134.1, 132.3, 127.6, 126.6, 126.4, 118.2, 96.1, 86.1, 71.9, 70.56, 70.55, 70.53, 70.46, 69.6, 59.0, 53.1, 38.0, 32.1. LRMS: m/z 524 ($[M + H]^+$), 546 ($[M + Na]^+$), 562 ($[M + K]^+$).

General Procedure for Alkylation Reactions. To a solution of macrocycle **13** (0.06 mmol) in dry MeCN (75 mL) were added a mesylate derivative (0.12 mmol) and Na_2CO_3 (0.12 mmol) . The resulting mixture was heated at reflux for 6 days and then filtered off. The filtrate was concentrated in vacuo, and the oily residue was partitioned between water (50 mL) and CH_2Cl_2 (50 mL). The aqueous layer was extracted with CH_2Cl_2 (2 × 25 mL). The organic phases were combined, dried over $MgSO_4$, filtered, and concentrated in vacuo. Purification of the sodium complexes was carried out using preparative RP-HPLC, leading to the desired compounds. The purity of the compounds was unambiguously established on the basis of the HPLC chromatogram.

Compound ***14***. Yield: 67%. ES$^+$-LRMS: m/z 692 ($[C_{40}H_{36}N_8O_4]^+$), 715 ($[M + Na]^+$).

Compound ***15***. Yield: 78%. ES$^+$-LRMS: m/z 1248 ($[C_{70}H_{72}N_8O_{10}S_2]^+$), 1271 ($[M + Na]^+$).

General Procedure for Ligand Deprotection. To a solution of a ligand diester precursor (0.04 mmol) in EtOH (15 mL) was added a 6 M NaOH aqueous solution (15 mL), and the mixture was stirred at room temperature for 1 h. The solvent was evaporated, and the aqueous phase was extended to 50 mL and then was extracted with EtOAc (2 × 25 mL). The aqueous phase was acidified with HCl (10%) to pH 1−2 and was extracted with CH_2Cl_2 (3 × 25 mL). The organic phases were combined, dried over Na_2SO_4, filtered, and concentrated in vacuo. Purifications of the crude material were carried out using preparative RP-HPLC, and the purities of the compounds were unambiguously established on the basis of the HPLC chromatogram (see the Supporting Information, Figure S1).

$\mathbf{L^1}$. Yield: 93%. HRMS: m/z 665.2595 ($[C_{38}H_{32}N_8O_4]^+$, $[M + H]^+$) (calcd m/z 665.2624).

$\mathbf{L^2}$. Yield: 87%. ES$^+$-LRMS: m/z 1220 ($[C_{68}H_{68}N_8O_{10}S_2]^+$), 1221 ($[M + H]^+$), 1243 ($[M + Na]^+$).

General Procedure for Synthesis of the Complexes. To a suspension of free ligand (0.04 mmol) and Na_2CO_3 (0.084) mmol) in dry MeCN (60 mL) was added $EuCl_3 \cdot 6H_2O$ (0.12 mmol). The solution was heated at reflux for 30 h under an inert atmosphere. The mixture was then cooled to room temperature and filtered off, and the filtrate was concentrated in vacuo. Purification of the complexes was carried out by preparative RP-HPLC, and the purities of the compounds were unambiguously established on the basis of the HPLC chromatogram (see the Supporting Information, Figure S1).

[Eu($\mathbf{L^1}$)][TFA]. Yield: 78%. ^{1}H NMR (500.10 MHz, D_2O): δ 18.16 (s, 2H), 9.59 (t, ^3J = 8 Hz, 2H), 9.33 (t, ^3J = 7.7 Hz, 2H), 9.08 (m, 4H), 8.73 (d, ^3J = 7.7 Hz, 2H), 7.9 (d, ^3J = 7.5 Hz, 2H), 7.38 (t, ^3J = 7.5 Hz, 2H), 7.2 (d, ^3J = 8 Hz, 2H), 3.14 (d, ^3J = 7.5 Hz, 2H), −0.57 (s, 2H), −7.84 (d, ^2J = 16 Hz, 2H), −11.09 (d, ^2J = 16 Hz, 2H), −13.14 (d, ^2J = 14.4 Hz, 2H), −15.84 (d, ^2J = 14.4 Hz, 2H). ^{19}F NMR (188.29 MHz, D_2O): δ −75.5. UV/vis: λ_{max} = 308 nm (ε = 18 000 L mol^{-1} cm^{-1}). HRMS: m/z 815.1584 ($[EuC_{38}H_{30}N_8O_4]^+$) (calcd m/z 815.1602).

[Eu($\mathbf{L^2}$)][TFA]. Yield: 90%. ^{1}H NMR (500.10 MHz, $CDCl_3$): δ 31.87 (s, 2H), 12.15 (s, 2H), 10.22 (s, 2H), 8.85 (s, 2H), 8.74 (s, 2H), 8.4 (s, 2H), 8.01 (d, ^3J = 7.8 Hz, 4H), 7.65 (d, ^3J = 7.8 Hz, 4H), 6.86 (s, 2H), 6.3 (s, 4H), 3.9−3.4 (m, 30H), 2.93 (s, 2H), −6.08 (s, 2H), −7.65 (s, 2H), −10.13 (s, 2H), −19.7 (s, 2H). ^{19}F NMR (188.29 MHz, $CDCl_3$): δ −74.9. UV/vis: λ_{max} = 308 (ε = 61 000 L mol^{-1} cm^{-1}) and 337 nm (ε = 53 000 L mol^{-1} cm^{-1}). HRMS: m/z 1373.3584 ($[EuC_{68}H_{68}N_8O_{10}S_2]^+$) (calcd m/z 1373.3712).

■ ASSOCIATED CONTENT

Supporting Information. Semipreparative HPLC analysis, optimized geometry for the lutetium complexes, Cartesian coordinates for all optimized geometries, and a low-temperature emission spectrum of [Eu$\mathbf{L^2}$][TFA] in MeTHF. This material is available free of charge via the Internet at http://pubs.acs.org.

■ AUTHOR INFORMATION

Corresponding Author

*E-mail: llamarque@cisbio.com (L.L.), olivier.maury@ens-lyon.fr (O.M.).

■ ACKNOWLEDGMENT

B.L.G. thanks the Pôle Scientifique de Modélisation Numérique (PSMN) at Ecole Normale Supérieure de Lyon for the computing facilities. We thank F. Albrieux, C. Duchamp, and N. Henriques from the Université de Lyon for assistance and access to the mass spectrometry facility.

■ REFERENCES

(1) For recent reviews, see: (a) Andraud, C.; Maury, O. *Eur. J. Inorg. Chem.* **2009**, 4357–4371. (b) Eliseeva, S. V.; Bünzli, J.-C. G. *Chem. Soc.*

Rev. **2010**, *39*, 189–227. (c) Ma, Y.; Wang, Y. *Coord. Chem. Rev.* **2010**, *254*, 972–990.

(2) (a) D'Aléo, A.; Pompidor, G.; Elena, B.; Vicat, J.; Baldeck, P. L.; Toupet, L.; Kahn, R.; Andraud, C.; Maury, O. *ChemPhysChem* **2007**, *8*, 2125–2132. (b) Picot, A.; D'Aléo, A.; Baldeck, P. L.; Grichine, A.; Duperray, A.; Andraud, C.; Maury, O. *J. Am. Chem. Soc.* **2008**, *130*, 1532–1533. (c) Law, G. L.; Wong, K.-L.; Man, C. W.-Y.; Wong, W.-T.; Tsao, S.-W.; Lam, M. H.-W.; Lam, P. K.-S. *J. Am. Chem. Soc.* **2008**, *130*, 3714–3715. (d) Kielar, F.; Congreve, A.; Law, G.-L.; New, E. J.; Parker, D.; Wong, L.-L.; Castreno, P.; De Mendoza, J. *Chem. Commun.* **2008**, 2435–2437. (e) Kielar, F.; Law, G.-L.; New, E. J.; Parker, D. *Org. Biomol. Chem.* **2008**, *6*, 2256–2258. (f) Law, G.-L.; Wong, K.-L.; Man, C. W.-Y.; Tsao, S.-W.; Wong, W.-T. *J. Biophoton.* **2009**, *2*, 718–724. (g) Kadjane, P.; Starck, M.; Camerel, F.; Hill, D.; Hildebrandt, N.; Ziessel, R.; Charbonniere, L. J. *Inorg. Chem.* **2009**, *48*, 4601–4603. (h) Eliseeva, S. V.; Auböck, G.; van Mourik, F.; Cannizzo, A.; Song, B.; Deiters, E.; Chauvin, A.-S.; Chergui, M.; Bünzli, J.-C. G. *J. Phys. Chem. B* **2010**, *114*, 2932–2937. (i) Shao, G.; Han, R.; Ma, Y.; Tang, M.; Xue, F.; Sha, Y.; Wang, Y. *Chem.—Eur. J.* **2010**, *16*, 8647–8651.

(3) (a) Kim, H. M.; Cho, B. R. *Acc. Chem. Res.* **2009**, *42*, 863–872. (b) He, G. S.; Tan, L.-S.; Zheng, Q.; Prasad, P. N. *Chem. Rev.* **2008**, *108*, 1245–1330. (c) Yuste, R. *Nat. Methods* **2005**, *2*, 902–904. (d) Mertz, J. *Curr. Opin. Neurobiol.* **2004**, *14*, 610–616. (e) Campagnola, P. J.; Loew, L. M. *Nat. Biotechnol.* **2003**, *21*, 1356–1360. (f) Zipfel, W. R.; Williams, R. M.; Webb, W. W. *Nat. Biotechnol.* **2003**, *21*, 1369–1377.

(4) (a) Moore, E. G.; Samuel, A. P. S.; Raymond, K. N. *Acc. Chem. Res.* **2009**, *42*, 542–552. (b) Bünzli, J.-C. G.; Comby, S.; Chauvin, A.-S.; Vandevyver, C. D. B. *J. Rare Earths* **2007**, *25*, 257–274. (c) Pandya, S.; Yu, J.; Parker, D. *Dalton Trans.* **2006**, 2757–2766. (d) Bünzli, J.-C. G. *Acc. Chem. Res.* **2006**, *39*, 53–61. (e) Gunlaugsson, T.; Leonard, J. P. *Chem. Commun.* **2005**, 3114–3131. (f) Faulkner, S.; Pope, S. J. A.; Burton-Pye, B. P. *Appl. Spectrosc. Rev.* **2004**, *39*, 1–35. (g) Parker, D. *Chem. Soc. Rev.* **2004**, *33*, 156–165. (h) Bünzli, J.-C. G.; Piguet, C. *Chem. Rev.* **2002**, *102*, 1897–1928. (i) Parker, D.; Dickins, R. S.; Puschmann, H.; Crossland, C.; Howard, J. A. K. *Chem. Rev.* **2002**, *102*, 1977–2010.

(5) Piszczek, G.; Maliwal, B. P.; Gryczynski, I.; Dattelbaum, J.; Lakowicz, J. R. *J. Fluoresc.* **2001**, *11*, 101–107.

(6) Werts, M. H. V.; Nerambourg, N.; Pélégry, D.; Le Grand, Y.; Blanchard-Desce, M. *Photochem. Photobiol. Sci.* **2005**, *4*, 531–538.

(7) (a) Fu, L.-M.; Wen, X.-F.; Ai, X.-C.; Sun, Y.; Wu, Y.-S.; Zhang J.-P.; Wang, Y. *Angew. Chem., Int. Ed.* **2005**, *44*, 747–750. (b) Hao, R.; Li, M.; Wang, Y.; Zhang, J.; Ma, Y.; Fu, L.; Wen, X.; Wu, Y.; Ai, X.; Zhang, S.; Wie, Y. *Adv. Funct. Mater.* **2007**, *17*, 3663–3669. (c) Xue, F.; Ma, Y.; Fu, L.; Hao, R.; Shao, G.; Tang, M.; Zhang, J.; Wang, Y. *Phys. Chem. Chem. Phys.* **2010**, *12*, 3195–3202.

(8) Picot, A.; Malvolti, F.; Le Guennic, B.; Baldeck, P. L.; Williams, J. A. G.; Andraud, C.; Maury, O. *Inorg. Chem.* **2007**, *46*, 2659–2665.

(9) D'Aléo, A.; Picot, A.; Baldeck, P. L.; Andraud, C.; Maury, O. *Inorg. Chem.* **2008**, *47*, 10269–10279.

(10) Chauvin, A.-S.; Gumy, F.; Imbert, D.; Bünzli, J.-C. G. *Spectrosc. Lett.* **2004**, *37*, 517–532.Erratum, 2007, *40*, 193.

(11) D'Aléo, A.; Allali, M.; Picot, A.; Baldeck, P. L.; Toupet, L.; Andraud, C.; Maury, O. *C. R. Chim.* **2010**, *13*, 681–690.

(12) (a) Alpha, B.; Lehn, J.-M.; Mathis, G. *Angew. Chem., Int. Ed.* **1987**, *26*, 266–267. (b) Sabbatini, N.; Guardigli, M.; Lehn, J.-M. *Coord. Chem. Rev.* **1993**, *123*, 201–228.

(13) (a) Mathis, G. *Clin. Chem.* **1993**, *39*, 1953–1959. (b) Mathis, G. *Clin. Chem.* **1995**, *41*, 1391–1397. (c) Mathis, G. *J. Biomol. Screen.* **1999**, *4*, 309–314.

(14) For selected recent examples, see: (a) Trinquet, E.; Fink, M.; Bazin, H.; Grillet, F.; Maurin, F.; Bourrier, E.; Ansanay, H.; Leroy, C.; Michaud, A.; Durroux, T.; Maurel, D.; Malhaire, F.; Goudet, C.; Pin J.-P.; Naval, M.; Hernout, O.; Chretien, F.; Chapleur, Y.; Mathis, G. *Anal. Biochem.* **2006**, *358*, 126–135. (b) Albizu, L.; Teppaz, G.; Seyer, R.; Bazin, H.; Ansanay, H.; Manning, M.; Mouillac, B.; Durroux, T. *J. Med. Chem.* **2007**, *50*, 4976–4985. (c) Maurel, D.; Comps-Agrar, L.; Brock, C.; Rives, M. L.; Bourrier, E.; Ayoub, M. A.; Bazin, H.; Tinel, N.; Durroux, T.; Prézeau, L.; Trinquet, E.; Pin, J.-P. *Nat. Methods* **2008**, *5*, 561–567. (d) Albizu, L.; Cottet, M.; Kralikova, M.; Stoev, S.; Seyer, R.; Brabet, I.; Roux, T.; Bazin, H.; Bourrier, E.; Lamarque, L.; Breton, C.; Rives, M.-L.; Newman, E.; Javitch, J.; Trinquet, E.; Manning, M.; Pin J.-P.; Mouillac, B.; Durroux, T. *Nat. Chem. Biol.* **2010**, *6*, 587–594.

(15) For selected examples, see: (a) Takalo, H.; Hemmilä; Sutela, T.; Latva, M. *Helv. Chim. Acta* **1996**, *79*, 789–801. (b) Chatterton, N.; Bretonnière, Y.; Pécaut, J.; Mazzanti, M. *Angew. Chem., Int. Ed.* **2005**, *44*, 7595–7598. (c) Gateau, C.; Mazzanti, M.; Pécaut, J.; Dunand, F. A.; Helm, L. *Dalton Trans.* **2003**, 2428–2433. (d) Nocton, G.; Nonat, A.; Gateau, C.; Mazzanti, M. *Helv. Chim. Acta* **2009**, *92*, 2257–2273. (e) Mato-Iglesias, M.; Roca-Sabio, A.; Palinkas, Z.; Esteban-Gomez, D.; Platas-Iglesias, C.; Toth, E.; De Blas, A.; Rodriguez-Blas, T. *Inorg. Chem.* **2008**, *47*, 7840–7851. (f) Roca-Sabio, A.; Mato-Iglesias, M.; Esteban-Gomez, D.; Toth, E.; De Blas, A.; Platas-Iglesias, C.; Rodriguez-Blas, T. *J. Am. Chem. Soc.* **2009**, *131*, 3331–3341. (g) Roca-Sabio, A.; Mato-Iglesias, M.; Esteban-Gomez, D.; De Blas, A.; Rodriguez-Blas, T.; Platas-Iglesias, C. *Dalton Trans.* **2011**, *40*, 384–392.

(16) (a) Huang, L.; Quada, J. C., Jr.; Lown, J. W. *Bioconjugate Chem.* **1995**, *6*, 21–33. (b) Storr, T.; Cameron, B. R.; Gossage, R. A.; Yee, H.; Skerlj, R. T.; Darkes, M. C.; Fricker, S. P.; Bridger, G. J.; Davies, N. A.; Wilson, M. T.; Maresca, K. P.; Zubieta, J. *Eur. J. Inorg. Chem.* **2005**, *13*, 2685–2697.

(17) Newkome, G. R.; Pappalardo, S.; Gupta, V. K.; Fronczek, F. R. *J. Org. Chem.* **1983**, *48*, 4848–4851.

(18) Sénéchal-David, K.; Hemeryck, A.; Tancrez, N.; Toupet, L.; Williams, J. A. G.; Ledoux, I.; Zyss, J.; Boucekkine, A.; Guégan, J.-P.; Le Bozec, H.; Maury, O. *J. Am. Chem. Soc.* **2006**, *128*, 12243–12255.

(19) We have checked that these longer bond lengths are not due to our calculation method. Indeed, using the same simulation parameters, the optimized geometry of Lu(tpatcn) fits well with the X-ray diffraction data.[15c]

(20) D'Aléo, A.; Picot, A.; Beeby, A.; Williams, J. A. G.; Le Guennic, B.; Andraud, C.; Maury, O. *Inorg. Chem.* **2008**, *47*, 10258–10268.

(21) (a) Werts, M. H. V.; Duin, M. A.; Hofstraat, J. W.; Verhoeven, J. W. *Chem. Commun.* **1999**, 799–800. (b) Yang, C.; Fu, L.-M.; Wang, Y.; Zhang, J.-P.; Wong, W.-T.; Ai, X.-C.; Qiao, Y.-F.; Zou, B.-S.; Gui, L.-L. *Angew. Chem., Int. Ed.* **2004**, *43*, 5010–5013.

(22) (a) Sabbatini, N.; Guardigli, M.; Manet, I.; Bolletta, F.; Ziessel, R. *Inorg. Chem.* **1994**, *33*, 955–959. (b) Havas, F.; Leygue, N.; Danel, M.; Mestre, B.; Galaup, C.; Picard, C. *Tetrahedron* **2009**, *65*, 7673−7686 and references cited therein.

(23) (a) Supkowski, R. M.; Horrocks, W. D. *Inorg. Chim. Acta* **2002**, *340*, 44. (b) Beeby, A.; Clarkson, I. M.; Dickins, R. S.; Faulkner, S.; Parker, D.; Royle, L.; de Sousa, A. S.; Williams, J. A. G.; Woods, M. *J. Chem. Soc., Perkin Trans. 2* **1999**, 493.

(24) Bünzli, J.-C. G.; Eliseeva, S. V . *Lanthanide Luminescence: Photophysical, Analytical and Biological Aspects*; Springer-Verlag: Berlin, 2010; published on the web July 15, 2010, DOI 10.1007/4243_2010_3.

(25) For selected examples, see: (a) Zucchi, G.; Scopelliti, R.; Pittet, P.-A.; Bünzli, J.-C. G.; Rogers, R. D. *J. Chem. Soc., Dalton Trans.* **1999**, 931–938. (b) Zucchi, G.; Scopelliti, R.; Bünzli, J.-C. G. *J. Chem. Soc., Dalton Trans.* **2001**, 1975–1985. (c) Kang, J. G.; Hong, J. P.; Yoon, S. K.; Bae, J. H.; Kim, Y. D. *J. Alloys Compd.* **2002**, *339*, 248–254. (d) Samuel, A. P. S.; Moore, E. G.; Melchior, M.; Xu, J.; Raymond, K. N. *Inorg. Chem.* **2008**, *47*, 7535–7544.

(26) Note that similar results are obtained using MeTHF at low temperature (see the Supporting Information, Figure S3).

(27) This conclusion is based on the hypothesis of a sensitization process mediated by an antenna effect from a charge-transfer excited state, as was already shown for related complexes.[20] Alternatively, given the electronic structure of $\mathbf{L}^2$, a photoinduced electron-transfer process could also be operative and would be consistent with the solvent and temperature dependence of the luminescence intensity.

(28) Werts, M. H. V.; Jukes, R. T. F.; Verhoeven, J. W. *Phys. Chem. Chem. Phys.* **2002**, *4*, 1542.

(29) Beeby, A.; Bushby, L. M.; Maffeo, D.; Williams, J. A. G. *J. Chem. Soc., Dalton Trans.* **2002**, 48–54.

(30) Details of the calculations can be found in several articles. See, for example, refs 20 and 28.

(31) Xu, C.; Webb, W. W. *J. Opt. Soc. Am. B* **1996**, *13*, 481–491.

(32) Picot, A.; Feuvrie, C.; Barsu, C.; Malvolti, F.; Le Guennic, B.; Le Bozec, H.; Andraud, C.; Toupet, L.; Maury, O. *Tetrahedron* **2008**, *64*, 399–411.

(33) Frisch, M. J.; Trucks, G. W.; Schlegel, H. B.; Scuseria, G. E.; Robb, M. A.; Cheeseman, J. R., Jr.; Vreven, J. A. T.; Kudin, K. N.; Burant, J. C.; Millam, J. M.; Iyengar, S. S.; Tomasi, J.; Barone, V.; Mennucci, B.; Cossi, M.; Scalmani, G.; Rega, N.; Petersson, G. A.; Nakatsuji, H.; Hada, M.; Ehara, M.; Toyota, K.; Fukuda, R.; Hasegawa, J.; Ishida, M.; Nakajima, T.; Honda, Y.; Kitao, O.; Nakai, H.; Klene, M.; Li, X.; Knox, J. E.; Hratchian, H. P.; Cross, J. B.; Adamo, C.; Jaramillo, J.; Gomperts, R.; Stratmann, R. E.; Yazyev, O.; Austin, A. J.; Cammi, R.; Pomelli, C.; Ochterski, J. W.; Ayala, P. Y.; Morokuma, K.; Voth, G. A.; Salvador, P.; Dannenberg, J. J.; Zakrzewski, V. G.; Dapprich, S.; Daniels, A. D.; Strain, M. C.; Farkas, O.; Malick, D. K.; Rabuck, A. D.; Raghavachari, K.; Foresman, J. B.; Ortiz, J. V.; Cui, Q.; Baboul, A. G.; Clifford, S.; Cioslowski, J.; Stefanov, B. B.; Liu, G.; Liashenko, A.; Piskorz, P.; Komaromi, I.; Martin, R. L.; Fox, D. J.; Keith, T.; Al-Laham, M. A.; Peng, C. Y.; Nanayakkara, A.; Challacombe, M.; Gill, P. M. W.; Johnson, B.; Chen, W.; Wong, M. W.; Gonzalez, C.; Pople, J. A. *Gaussian 03*, revision D.01; Gaussian, Inc.: Wallingford, CT, 2004.

(34) Adamo, C.; Barone, V. *J. Chem. Phys.* **1999**, *110*, 6158–6169.

(35) Dolg, M.; Stoll, H.; Preuss, H. *Theor. Chem. Acc.* **1993**, *85* 441–450.

(36) Dunning, T. H., Jr.; Hay, P. J. In *Modern Theoretical Chemistry*; Schaefer, H. F., III, Ed.; Plenum: New York, 1976; Vol. 3, pp 1−28.